ANALYSIS AND SIMULATION OF THE VARIOUS GENERATORS USED IN WIND SYSTEMS

L. ABDELHAMID, H. AMIMEUR
LEB-Research Laboratory, Department of Electrical Engineering, University of Batna,
Street Chahid Mohamed El hadi Boukhlouf, 05000, Batna, Algeria
E-mail: abdelhamidenergie@yahoo.fr; amimeurhocine2002@yahoo.fr

L. BAHMED
Laboratory of Research in Industrial Prevention (LRPI),
Industrial Health and Safety Institute, University of Batna, Algeria

Abstract: *The world's energy consumption grows unceasingly, raising important questions about the problem of global warming due to greenhouse gases (GHG), on the one hand, and to the exhaustion of the fossil resources, on the other one. Given this awareness, an economic development that abides by the environmental requirements is absolutely necessary. Wind power is one of the most promising renewable energies. It is within this context that this paper attempts to study the different configurations and performances of the most used generators in wind systems.*

Key words: *Various Generators, IG, DSIG, DFIG, PSMG, Simulation.*

1. Introduction

The search for a lasting development that is complying with the environmental requirements and the imminent exhaustion of fossil energies have contributed to the development of renewable energies in general and wind energy in particular [1]. Within this context, this research work deals with the various generators used in the field of aerogenerators. A classification approach to the various generators used in wind systems will be introduced, and the main configuration of the fixed speed system and that of the variable speed one will be described. The mathematical models and the simulation of the induction generator (IG), the dual-stator windings induction generator (DSIG), the doubly fed induction generator (DFIG) as well as the permanent magnet synchronous generator (PSMG) will be dealt with in details.

2. Induction generator

2. 1. Mathematical model

The mathematical model of the induction generator in the quasi-stationary reference frame (α-β) are given as [2-4]

$$[B][U] = [A][I] + \omega_r [C][I] + [L]\dot{[I]} \tag{1}$$

with,

$[U] = \begin{bmatrix} v_{\alpha s} & v_{\beta s} & 0 & 0 \end{bmatrix}^T$;

$[I] = \begin{bmatrix} i_{\alpha s} & i_{\beta s} & i_{\alpha r} & i_{\beta r} \end{bmatrix}^T$ and $\dot{[I]} = \frac{d}{dt}[I]$;

$[B] = diag\begin{bmatrix} -1 & -1 & 0 & 0 \end{bmatrix}$;

$[A] = diag\begin{bmatrix} r_s & r_s & r_r & r_r \end{bmatrix}$;

$$[C] = \begin{bmatrix} 0 & 0 & 0 & 0 \\ 0 & 0 & 0 & 0 \\ 0 & L_m & 0 & L_r \\ -L_m & 0 & -L_r & 0 \end{bmatrix};$$

$$[L] = \begin{bmatrix} L_{\alpha s} & L_{\alpha\beta} & L_{m\alpha} & L_{\alpha\beta} \\ L_{\alpha\beta} & L_{\beta s} & L_{\alpha\beta} & L_{m\beta} \\ L_{m\alpha} & L_{\alpha\beta} & L_{\alpha r} & L_{\alpha\beta} \\ L_{\alpha\beta} & L_{m\beta} & L_{\alpha\beta} & L_{\beta r} \end{bmatrix}.$$

where,

r_s and r_r are respectively the per phase stator resistance and the per phase rotor resistance;

$L_{\alpha s}$, $L_{\beta s}$, $L_{\alpha r}$ and $L_{\beta r}$ are respectively the direct and quadrature of the total stator and rotor inductances;

ω_r is the rotor electrical angular speed;

$v_{\alpha s}$ and $i_{\alpha s}$ are respectively the "α" components of the stator voltages and currents;

$v_{\beta s}$ and $i_{\beta s}$ are respectively the "β" components of the stator voltages and currents;

$i_{\alpha r}$ and $i_{\beta r}$ are respectively the "α" and "β" components of the rotor currents;

L_m is the magnetizing inductance;

That under linear magnetic conditions $L_{\alpha\beta} = 0$, $L_{m\alpha} = L_{m\beta} = L_m$, $L_{\alpha s} = L_{\beta s}$ and $L_{\alpha r} = L_{\beta r}$.

The saturation effect is taken into account by the expression of the magnetizing inductance L_m with respect to the magnetizing current i_m defined as [5]

$$i_m = \sqrt{\left(i_{\alpha s} + i_{\alpha r}\right)^2 + \left(i_{\beta s} + i_{\beta r}\right)^2} \tag{2}$$

To express L_m with respect to i_m, we use a polynomial approximation is given by

$$L_m = 0.3308 - 0.0099 i_m - 0.0074 i_m^2 + 0.0006 i_m^3 \tag{3}$$

The electromagnetic torque is evaluated as [6-8]

$$T_{em} = \frac{3}{2} PL_m \left(i_{\beta s} i_{\alpha r} - i_{\alpha s} i_{\beta r} \right) \quad (4)$$

P is number of pole pairs.
The mechanical equation which remains the same for all generators is described as

$$J \frac{d\Omega}{dt} = T_{sh} - T_{em} \quad (5)$$

where,
Ω is the mechanical speed ($\Omega = \omega_r/P$);
T_{sh} is the shaft torque;
J is the moment of inertia.

2. 2. Resistive-inductive load model

General resistive-inductive passive load is represented in the quasi-stationary reference frame as the IG with the following equations

$$\begin{cases} pv_{\alpha s} = (1/C)(i_{\alpha s} - i_{\alpha sL}) \\ pi_{\alpha sL} = (1/L_L)(v_{\alpha s} - R_L i_{\alpha sL}) \\ pv_{\beta s} = (1/C)(i_{\beta s} - i_{\beta sL}) \\ pi_{\beta sL} = (1/L_L)(v_{\beta s} - R_L i_{\beta sL}) \end{cases} \quad (6)$$

where,
p denotes differentiation *w.r.t* time;
$i_{\alpha sL}$ and $i_{\beta sL}$ are respectively the "α" and "β" components of the currents flowing into excitation capacitor;
C is the excitation capacitance;
R_L is the load resistance;
L_L is the load inductance.

2. 3. Simulation results and discussion

The simulations in this paper have been developed in MATLAB/SIMULINK® environment. In the model the prime mover speed and the excitation capacitance are fixed at Ω_r=157.5*rad/s* and C=62μ*F/phase* respectively. The induction generator parameters used in the simulation are given in the Appendix.
Figs. 1, 2 and 3 show the variation of the stator voltage, the stator current and the magnetizing current of the induction generator. At t = 1.5*s*, the three-phase star load (resistive-inductive load (R_L = 150Ω and L_L = 500*mH*)) is applied.
Inserting the load leads to a decrease of the level of all the IG characteristics in comparison with those observed without a load (prior to inserting it), which are 8.18% at the level of the stator voltage (Fig. 1), 6.66% of the stator current (Fig. 2) and 16.82% of the magnetization current (Fig. 3). This is essentially due to the demagnetization of the machine and to the lack of reactive energy which is necessary for both magnetizing the machine and supplying the load, notably the one that is inductive and energy consuming, and it is up to the excitation capacitors to satisfy and share the energy that they produce between the two consumers of the reactive power. Fig. 4 shows the variation of the load current at resistive-inductive load, which stabilizes at 1.34*A*.

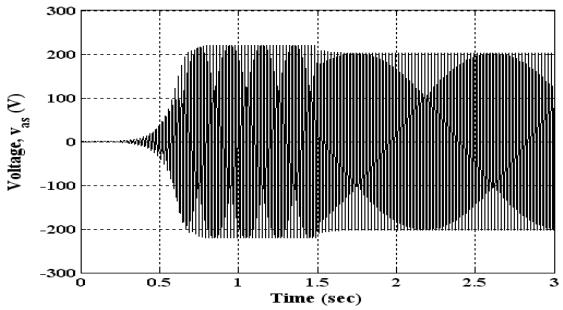

Fig. 1. Variation of the IG voltage (v_{as}(*V*)) at resistive-inductive load.

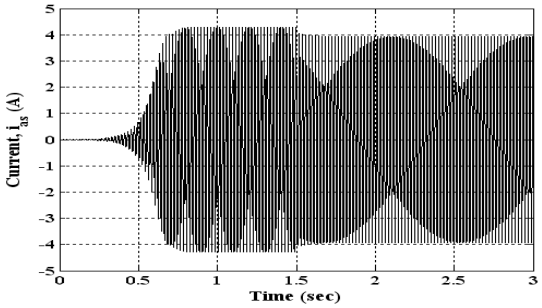

Fig. 2. Variation of the IG current (i_{as}(*A*)) at resistive-inductive load.

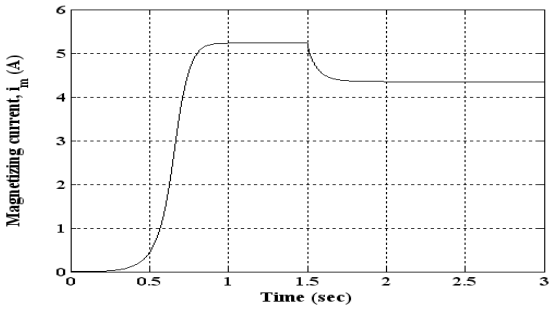

Fig. 3. Variation of the IG magnetizing current (i_m(*A*)) at resistive-inductive load.

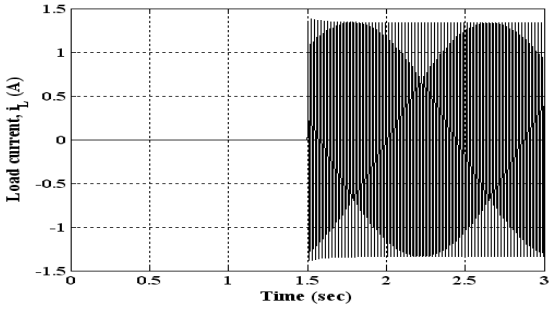

Fig. 4. Variation of the IG load current (i_L(*A*)) at resistive-inductive load.

3. Dual-stator windings induction generator

3. 1. Mathematical model

The mathematical model of the dual-stator windings induction generator in the synchronous reference frame (*d*-*q*) is given as [9, 11]

$$[B][U]=[A][I]+\omega_{sl}[C][I]+[L]\dot{[I]} \tag{7}$$

with,

$[U]=\begin{bmatrix} v_{d1} & v_{q1} & v_{d2} & v_{q2} & v_{dr} & v_{qr}\end{bmatrix}^T$;

$[I]=\begin{bmatrix} i_{d1} & i_{q1} & i_{d2} & i_{q2} & i_{dr} & i_{qr}\end{bmatrix}^T$;

$[B]=diag[1 \;\; 1 \;\; 1 \;\; 1 \;\; 0 \;\; 0]$;

[*A*], [*C*] and [*L*] are respectively given by matrices (8), (9) and (10), where L_{ld}, L_{lq} and ω_{sl} are defined as:

$L_{ld} = L_{lm} + L_{md}$, $L_{lq} = L_{lm} + L_{mq}$ and $\omega_{sl} = \omega_e - \omega_r$;

ω_e is the speed of the synchronous reference frame;

v_{d1}, v_{d2} and i_{d1}, i_{d2} are respectively the "*d*" components of the stator voltages and currents;

v_{q1}, v_{q2} and i_{q1}, i_{q2} are respectively the "*q*" components of the stator voltages and currents;

v_{dr}, i_{dr} and ψ_{dr} are respectively the "*d*" components of the rotor voltage, current and flux linkage;

v_{qr}, i_{qr} and ψ_{qr} are respectively the "*q*" components of rotor voltage, current and flux linkage;

r_1, r_2 and r_r are respectively the per phase stator resistance and the per phase rotor resistance;

L_{md} and L_{mq} are respectively the direct and quadrature magnetizing inductance.

That under linear magnetic conditions $L_{md} = L_{mq} = L_m$ and $L_{dq} = 0$.

L_m is the steady state saturated inductance and is given by [10]

$$L_m = 0.1406 + 0.0014 i_m - 0.0012 i_m^2 + 0.00005 i_m^3 \tag{11}$$

The magnitude of the magnetizing current $|i_m|$ is calculated as

$$i_m = \sqrt{\left(-i_{d1} - i_{d2} + i_{dr}\right)^2 + \left(-i_{q1} - i_{q2} + i_{qr}\right)^2} \tag{12}$$

The electromagnetic torque is evaluated as [11, 12]

$$T_{em} = \frac{3}{2} P \frac{L_m}{L_r}\left[\left(i_{q1} + i_{q2}\right)\psi_{dr} - \left(i_{d1} + i_{d2}\right)\psi_{qr}\right] \tag{13}$$

3. 2. Resistive-inductive load model

General resistive-inductive passive load is represented in the synchronous reference frame as the DSIG with the following equations

$$\begin{cases} pv_{d1} = \left(1/C_{sh1}\right)\left(i_{d1} - i_{d1L}\right) + \omega_e v_{q1} \\ pi_{d1L} = \left(1/L_1\right)\left(v_{d1} - R_1 i_{d1L} + \omega_e L_1 i_{q1L}\right) \end{cases} \tag{14}$$

$$[A]=\begin{bmatrix} -r_1 & -\omega_e(L_{l1}+L_{lq}) & -\omega_e L_{dq} & \omega_e L_{lq} & 0 & -\omega_e L_{mq} \\ -\omega_e(L_{l1}+L_{ld}) & -r_1 & -\omega_e L_{ld} & -\omega_e L_{dq} & \omega_e L_{md} & 0 \\ \omega_e L_{dq} & \omega_e L_{lq} & -r_2 & -\omega_e(L_{l2}+L_{lq}) & 0 & -\omega_e L_{mq} \\ -\omega_e L_{ld} & \omega_e L_{dq} & -\omega_e(L_{l2}+L_{ld}) & -r_2 & \omega_e L_{md} & 0 \\ 0 & 0 & 0 & 0 & r_r & 0 \\ 0 & 0 & 0 & 0 & 0 & r_r \end{bmatrix} \tag{8}$$

$$[C]=\begin{bmatrix} 0 & 0 & 0 & 0 & 0 & 0 \\ 0 & 0 & 0 & 0 & 0 & 0 \\ 0 & 0 & 0 & 0 & 0 & 0 \\ 0 & 0 & 0 & 0 & 0 & 0 \\ 0 & L_{mq} & 0 & L_{mq} & 0 & L_{lr}+L_{mq} \\ -L_{md} & 0 & -L_{md} & 0 & L_{lr}+L_{md} & 0 \end{bmatrix} \tag{9}$$

$$[L]=\begin{bmatrix} -(L_{l1}+L_{ld}) & 0 & -L_{ld} & -L_{dq} & L_{md} & 0 \\ 0 & -(L_{l1}+L_{lq}) & L_{dq} & -L_{lq} & 0 & L_{mq} \\ -L_{ld} & L_{dq} & -(L_{l2}+L_{ld}) & 0 & L_{md} & 0 \\ -L_{dq} & -L_{lq} & 0 & -(L_{l2}+L_{lq}) & 0 & L_{mq} \\ -L_{md} & 0 & -L_{md} & 0 & L_{lr}+L_{md} & 0 \\ 0 & -L_{mq} & 0 & -L_{mq} & 0 & L_{lr}+L_{mq} \end{bmatrix} \tag{10}$$

$$\begin{cases} pv_{q1} = (1/C_{sh1})(i_{q1} - i_{q1L}) - \omega_e v_{d1} \\ pi_{q1L} = (1/L_1)(v_{q1} - R_1 i_{q1L} - \omega_e L_1 i_{d1L}) \end{cases} \quad (15)$$

$$\begin{cases} pv_{d2} = (1/C_{sh2})(i_{d2} - i_{d2L}) + \omega_e v_{q2} \\ pi_{d2L} = (1/L_2)(v_{d2} - R_2 i_{d2L} + \omega_e L_2 i_{q2L}) \end{cases} \quad (16)$$

$$\begin{cases} pv_{q2} = (1/C_{sh2})(i_{q2} - i_{q2L}) - \omega_e v_{d2} \\ pi_{q2L} = (1/L_2)(v_{q2} - R_2 i_{q2L} - \omega_e L_2 i_{d2L}) \end{cases} \quad (17)$$

where,
C_{sh1} and C_{sh2} are respectively the excitation capacitance connected the dual stator windings set *I* and *II*;
R_1 and R_2 are respectively the load resistances connected across the windings set *I* and *II*;
L_1 and L_2 are respectively the load inductances connected across the windings set *I* and *II*;
i_{d1L}, i_{d2L} and i_{q1L}, i_{q2L} are respectively the "*d*" and "*q*" components of the load current.

3. 3. Simulation results and discussion

In the model the prime mover speed (Ω_r) and the excitation capacitance are fixed at 157*rad/s*, and C_{sh1} = C_{sh2} = 40$\mu F/phase$ respectively. The dual-stator windings induction generator parameters used in the simulation are given in the Appendix.
Figs. 5, 6 and 7 show the variation of the stator voltage, the stator current and the magnetizing current of the dual-stator windings of induction generator sets *I* respectively. Figs 8 and 9 show the variation of the load current of the DSIG sets *I* and *II* respectively.
At t = 3*s*, the three-phase star load (resistive-inductive load ($R_1 = R_2 = 200\Omega$ and $L_1 = L_2 = 0.05H$)) is applied, the generated voltage, the stator current and the magnetizing current decrease respectively to 35.26%, 34.98% and 42.58% regarding to the values at no load. Application of the load, as the case of classical induction generator, causes the decrease of the voltage generated by the decrease of the magnetizing current. Furthermore, the introduce of an inductive load generate more important decrease of reactive power.

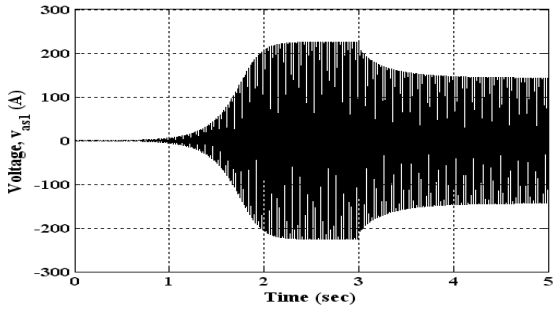

Fig. 5. Variation of the DSIG voltage ($v_{as1}(V)$ phase s_{a1}) at resistive-inductive load.

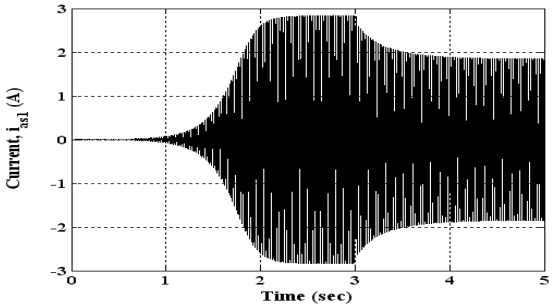

Fig. 6. Variation of the DSIG current ($i_{as1}(A)$ phase s_{a1}) at resistive-inductive load.

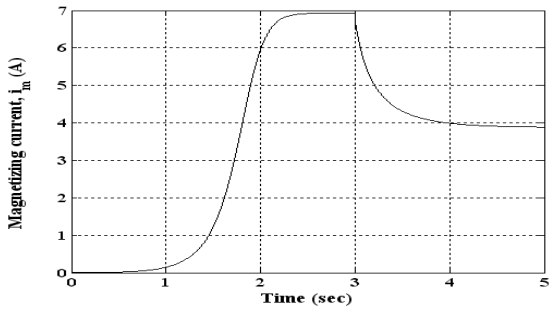

Fig. 7. Variation of the DSIG magnetizing current ($i_m(A)$ phase s_{a1}) at resistive-inductive load.

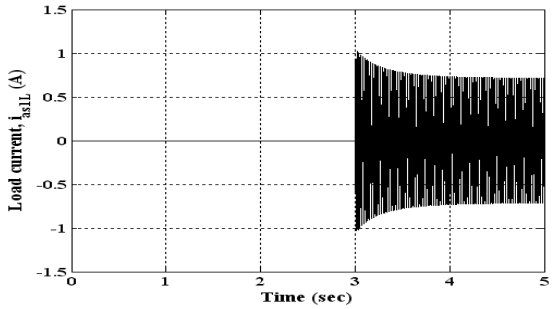

Fig. 8. Variation of the DSIG load current ($i_{as1L}(A)$ phase s_{a1}) at resistive-inductive load.

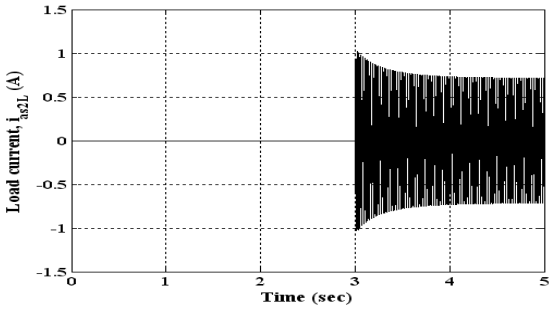

Fig. 9. Variation of the DSIG load current ($i_{as2L}(A)$ phase s_{a2}) at resistive-inductive load.

4. Doubly fed windings induction generator

4. 1. Mathematical model

The mathematical model of the doubly fed induction generator in the synchronous reference frame (*d-q*) are given as [13-15]

$$[B][U]=[A][I]+\omega_{sl}[C][I]+[L]\dot{[I]} \tag{18}$$

with, $[U]=\begin{bmatrix} v_{ds} & v_{qs} & v_{dr} & v_{qr}\end{bmatrix}^T$;

$[I]=\begin{bmatrix} i_{ds} & i_{qs} & i_{dr} & i_{qr}\end{bmatrix}^T$; $[B]=diag[1 \quad 1 \quad 1 \quad 1]$;

$$[A]=\begin{bmatrix} -r_s & \omega_e L_s & 0 & -\omega_e L_m \\ -\omega_e L_s & -r_s & \omega_e L_m & 0 \\ 0 & 0 & -r_r & 0 \\ 0 & 0 & 0 & -r_r \end{bmatrix};$$

$$[C]=\begin{bmatrix} 0 & 0 & 0 & 0 \\ 0 & 0 & 0 & 0 \\ 0 & L_m & 0 & -L_r \\ -L_m & 0 & L_r & 0 \end{bmatrix};$$

$$[L]=\begin{bmatrix} -L_s & 0 & L_m & 0 \\ 0 & -L_s & 0 & L_m \\ -L_m & 0 & L_r & 0 \\ 0 & -L_m & 0 & L_r \end{bmatrix}.$$

where, L_s and L_r are respectively the total stator and rotor inductances;

The electromagnetic torque is expressed as [16, 17]

$$T_{em}=\frac{3}{2}P\frac{L_m}{L_s}\left(i_{qr}\psi_{ds}-i_{dr}\psi_{qs}\right) \tag{19}$$

4. 2. Resistive load model

General resistive passive load is represented in the synchronous reference frame (*d-q*) as the DFIG with the following equations

$$\begin{cases} v_{ds}=R_L i_{ds} \\ v_{qs}=R_L i_{qs} \end{cases} \tag{20}$$

4. 3. Simulation results and discussion

In the model the prime mover speed (Ω_r) is fixed at 106*rad/s*. The DFIG parameters used in the simulation are given in the Appendix.

Figs. 10, 11, 12 and 13 show respectively the variation of the stator voltage, the rotor voltage, the stator current and the rotor current of the doubly fed induction generator outflows on a resistive load ($R_L = 100\Omega$).

At the start, the generated stator voltage ($v_{as}(V)$) and stator current ($i_{as}(A)$) increase in an exponential way during a few fractions of milliseconds, then they respectively stabilize at 217.8*V* and at 2.176*A* and at a rate of flow totally established at $t = 0.158s$, then they continue their progress with constant amplitudes knowing that the frequency is kept constant.

The rotor voltage ($v_{ar}(V)$) progresses in a sinusoidal way and with amplitude that is equal to $12\sqrt{2}V$ and in a frequency periodic of 2*Hz*. The rotor current ($i_{ar}(A)$) stabilizes right at the second alternation. Then, it evolves in a sinusoidal way with constant amplitude that is approximately at 9.05*A*, and with a frequency that is identical to that of the rotor voltage.

The various characteristics of the DFIG functioning show that the transitional speed is of a very short duration.

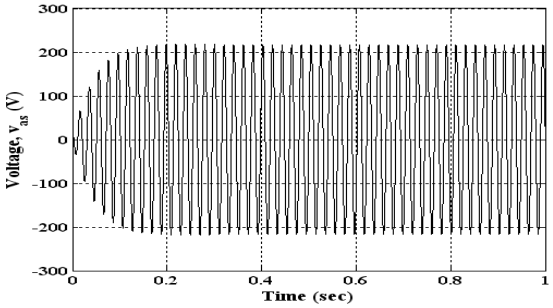

Fig. 10. Variation of the DFIG stator voltage ($v_{as}(V)$) at resistive load.

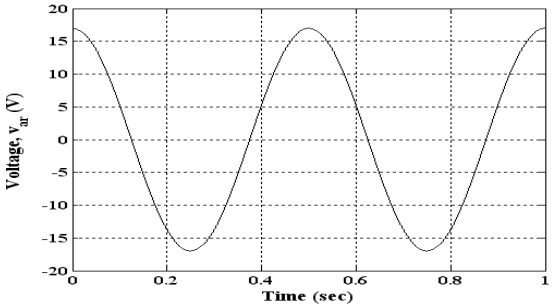

Fig. 11. Variation of the DFIG rotor voltage ($v_{ar}(V)$) at resistive load.

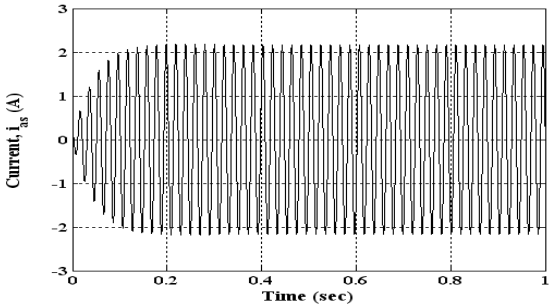

Fig. 12. Variation of the DFIG stator current ($i_{as}(A)$) at resistive load.

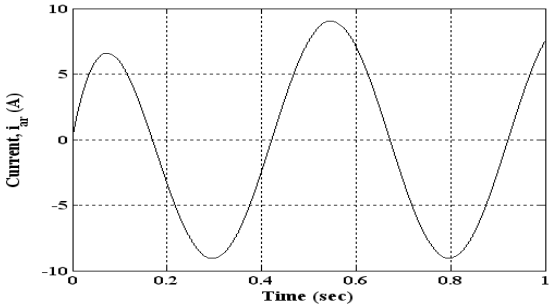

Fig. 13. Variation of the DFIG rotor current ($i_{ar}(A)$) at resistive load.

5. Permanent magnet synchronous generator

5. 1. Mathematical model

The mathematical model of the permanent magnet synchronous generator in the rotor frame (*x-y*) is given as [18, 19]

$$[B][U]=[A][I]+\omega_r[C][I]+[L]\dot{[I]}+\omega_r[D]\varphi_f \qquad (21)$$

with,

$$[U]=\begin{bmatrix} v_{xs} & v_{ys}\end{bmatrix}^T;$$

$$[I]=\begin{bmatrix} i_{xs} & i_{ys}\end{bmatrix}^T;$$

$$[B]=diag[1 \;\; 1];$$

$$[A]=[-r_s \;\; -r_s];$$

$$[L]=diag\begin{bmatrix}-L_{xs} & -L_{ys}\end{bmatrix};$$

$$[D]=[0 \;\; 1]^T;$$

$$[C]=\begin{bmatrix} 0 & -L_{ys} \\ -L_{xs} & 0\end{bmatrix};$$

where,

v_{xs}, v_{ys} and i_{xs}, i_{ys} are respectively the "*x*" and "*y*" components of the stator voltages and currents;

L_{xs} and L_{ys} are respectively the direct and quadrature of the total stator inductances;

φ_f is the flux produced by the permanent magnets.

The electromagnetic torque is expressed as [20, 21]

$$T_{em}=\frac{3}{2}P\left[\left(L_{xs}-L_{ys}\right)i_{xs}i_{ys}+\varphi_f i_{ys}\right] \qquad (22)$$

5. 2. Resistive-inductive load model

General resistive-inductive passive load is represented in the rotor frame (*x-y*) as the PMSG with the following equations

$$\begin{bmatrix}0\\0\end{bmatrix}=\begin{bmatrix}-\left(r_s+R_L\right) & -\omega_r L_{ys}\\ \omega_r L_{xs} & -\left(r_s+R_L\right)\end{bmatrix}\begin{bmatrix}i_{xs}\\ i_{ys}\end{bmatrix}+\begin{bmatrix}0\\ \varphi_f\end{bmatrix}$$
$$\begin{bmatrix}-\left(L_{xs}+L_L\right) & 0\\ 0 & -\left(L_{ys}+L_L\right)\end{bmatrix}\frac{d}{dt}\begin{bmatrix}i_{xs}\\ i_{ys}\end{bmatrix} \qquad (23)$$

with,

$$\begin{cases} v_{xs}=R_L i_{xs}+L_L\dfrac{d}{dt}i_{xs}\\ v_{qs}=R_L i_{ys}+L_L\dfrac{d}{dt}i_{ys}\end{cases} \qquad (24)$$

5. 3. Simulation results and discussion

In the model the prime mover speed (Ω_r) is fixed at 314*rad/s*. The permanent magnet synchronous generator parameters used in the simulation are given in the Appendix.

Figs. 14, 15, 16 and 17 show the variation of the stator voltage, the stator current, the direct stator current and the quadrature stator current of the permanent magnet synchronous generator outflows on a resistive-inductive load ($R_L = 42\Omega$ and $L_L = 0.159H$). The results achieved demonstrate clearly that:

The current following the ($i_{xs}(A)$) direct axis stabilizes at $-0.15A$ staring from $t = 0.051s$. The in squaring one is $i_{ys} = 7.37A$ when beyond $t = 0.035s$. This leads us to conclude that the duration of the transitional speed is very short.

The stator current ($i_{as}(A)$) which moves through the load takes a sinusoidal form and evolves in a uniform way and with a constant amplitude starting from the second alternation ($t = 0.025s$), its utmost value is equal to $7.37A$.

The stator voltage ($v_{as}(V)$) reaches its maximal value of $482.6V$ at $t = 0.022s$ (second period), and continues its evolution in exactly the same way as the stator current ($i_{as}(A)$).

The stator current ($i_{as}(A)$) is out of phase to the rear in comparison with the voltage, which is due to the presence of the inductive charge and also to the inductive nature of the machine.

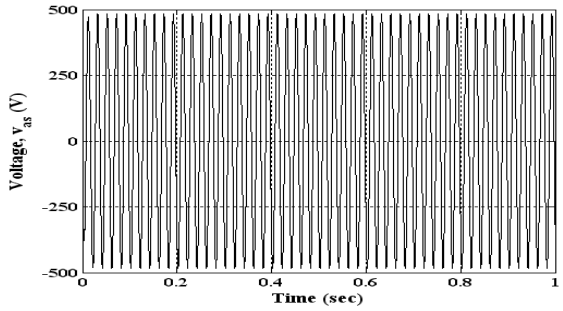

Fig. 14. Variation of the PSMG voltage ($v_{as}(V)$) at resistive-inductive load.

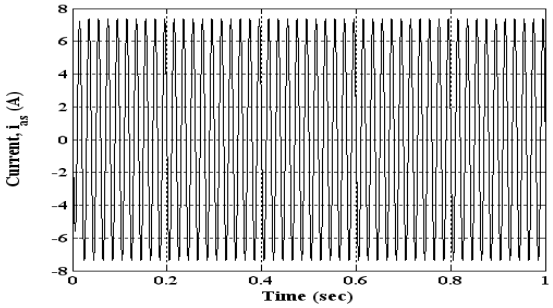

Fig. 15. Variation of the PSMG current ($i_{as}(A)$) at resistive-inductive load.

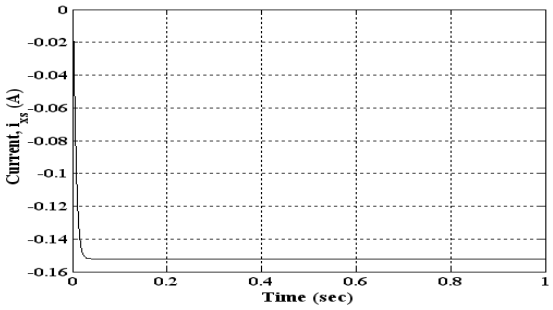

Fig. 16. Variation of the PSMG direct stator current ($i_{xs}(A)$) at resistive-inductive load.

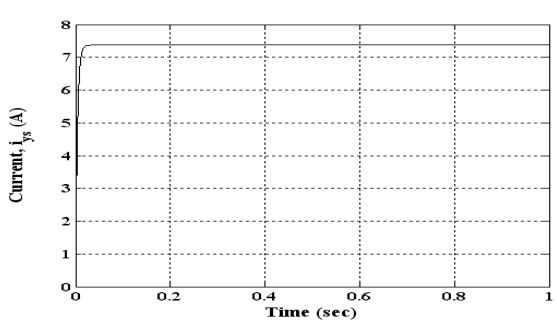

Fig. 17. Variation of the PSMG quadrature stator current ($i_{ys}(A)$) at resistive-inductive load.

6. Interpretation

Considering the simulation tasks done during the last years within the LEB research laboratory on the various generators previously studied, we can conclude that the induction generators constitute 85% of the wind applications, for a power range between $100kW$ and $1MW$. The dual-stator windings induction generator, dealt with only recently, constitute a serious rival to the induction generator. The doubly fed induction generator is widespread in the great power range. It constitutes, along with the permanent magnet synchronous generator, one of the two competing solutions in variable speed wind generators.

7. Conclusion

This paper has outlined the results achieved by the simulation of the various generators that are most commonly used in the aerodynamic conversion systems that function autonomously and which outflow on static charges.
The latter influence the generators which work with a fixed speed (IG and DSIG), because it is up to the excitation capacities to share the reactive energy that they produce between the load, notably the inductive one, and for the magnetization of the machine. Conversely, electrical generators working with a variable speed (DFIG and PSMG) remain unchanged with regard to the load.
The field of renewable energies, notably wind energies, is a new opportunity for research in electrical engineering. These research works will be fruitful and multidisciplinary enough to meet the requirements of these complex systems.

8. Appendix

The machine parameters used in the simulation are as follows:

1. IG parameters:
   - Stator resistance $r_s = 3.38\Omega$;
   - Stator leakage inductance $L_{\alpha s} = L_{\beta s} = 0.324H$;
   - Rotor resistance $r_r = 3.38\Omega$;
   - Rotor leakage inductance $L_{\alpha r} = L_{\beta r} = 0.324H$;
   - Moment of inertia $J = 0.005Kg.m^2$;
   - Number of poles pair $P = 2$.
2. DSIG parameters:
   - Stator resistances per-phase (winding set *I* and *II*) $r_1 = r_2 = 1.9\Omega$;
   - Stator leakage inductances per-phase (winding set *I* and *II*) $L_{l1} = L_{l2} = 0.0132H$;
   - Rotor per-phase resistance $r_r = 2.1\Omega$;
   - Rotor per-phase leakage inductance $L_{lr} = 0.0132H$;
   - Common mutual leakage inductance $L_{lm} = 0.011H$;
   - Moment of inertia $J = 0.038Kg.m^2$;
   - Number of poles pair $P = 2$.
3. DFIG parameters:
   - Stator resistance $r_s = 0.95\Omega$;
   - Stator leakage inductance $L_s = 0.094H$;
   - Rotor resistance $r_r = 1.8\Omega$;
   - Rotor leakage inductance $L_r = 0.088H$;
   - Mutual leakage inductance $L_m = 0.082H$;
   - Moment of inertia $J = 0.1Kg.m^2$;
   - Number of poles pair $P = 3$.
4. PSMG parameters:
   - Stator resistance $r_s = 0.6\Omega$;
   - Direct stator leakage inductance $L_{xs} = 0.0014H$;
   - Quadrature stator leakage inductance $L_{ys} = 0.0028H$;
   - Flux produced by the permanent magnets $\varphi_f = 1Wb$;
   - Number of poles pair $P = 1$.

References

1. Abdelhamid L., Abdessemed R., Amimeur H., Merabet E.: *Etude des performances des génératrices utilisées dans les systèmes éoliens*. In: Proceedings of the International Conference on Renewable Energy ICRE'07, Univ. Bejaia, Algeria, Nov. 25-27, 2007, p.1-6.
2. Hallenius K.E., Vas P., Brown J.E.: *The analysis of a saturated self-excited asynchronous generator*. In: IEEE Tans. Energy Convers., Vol. 6, No. 2, June 1991, p. 336-341.
3. Kishore A., Prassad R.C., Karan B.M.: *Matlab simulink based dq modelling dynamic characteristics of three phase self-excited induction generator*. In: Progress Electromagnetics Research Symposium, Cambridge, USA, Mar. 26-29, 2006, p. 312-316.
4. Singh B., Shilpakar L.B.: *Analysis of a novel solid state voltage regulator for a self-excited induction generator during balanced and unbalanced faults.* In: IEE Proc.-Gener. Transm. Distrib., Vol. 145, No. 6, Nov. 1998, p. 50-57.
5. Idjdarene K., Rekioua D., Rekioua T., Tounzi A.: *Vector control an autonomous induction generator taking saturation effect into account.* In: ScienceDirect, Elsevier, Energy Conversion and Management 49, 2008, p. 2609-2917.

6. Farret F.A., Palle B., Simões M.G.: *Full expandable model of parallel self-excited induction generators.* In: IEE Proc.-Electr. Power Appl., Vol. 52, No. 1, Jan. 2005, p. 96-102.
7. Aouzellag D., Ghedamsi K., Amimeur H., Taraft S.: *Improvement of the starting and braking times of an induction motor including magnetic saturation.* In: JEE Journal Elec. Engineering, Vol. 8, No. 4, 2008, Art. 14.
8. Palle B., Simões M.G., Farret F.A.: *Dynamic simulation and analysis of parallel self-excited induction generator for islanded wind farm systems.* In: IEEE Tans. Ind. Applicat. Vol. 41, No. 4, July/Aug. 2005, p. 1099-1106.
9. Singh G.K., Yadav K.B., Saini R.P.: *Analysis of a saturated multi-phase (six phase) self-excited induction generator.* In: Int. Journal Emerging Elec. Power Syst., Berkeley Electronic press, Vol. 7, No. 2, 2006, p. 1-21.
10. Singh G.K., Yadav K.B., Saini R.P.: *Modeling and analysis of multi-phase (six phase) self-excited induction generator.* In: Proc. IEEE Conf. ICEMS'2005, China, 2005, p. 1922-1927.
11. Amimeur H., Abdessemed R., Aouzellag D., Merabet E., Hamoudi F.: *Modeling and Analysis of Dual-Stator Windings Self-Excited Induction Generator.* In: JEE Journal Elec. Engineering, Vol. 8, No. 3, 2008, Art. 3.
12. Singh G.K.: *Modeling and experimental analysis of a self-excited six phase induction generator for stand-alone renewable energy generation.* In: ScienceDirect, Elsevier, Renewable Energy, 2007, p. 1-17.
13. Aouzellag D., Ghedamsi K., Berkouk E.M.: *Network power flux control of wind generator.* In: ScienceDirect, Elsevier, Renewable Energy 34, 2009, p. 615-622.
14. Pena R., Clare J.C., Asher G.M.: *A doubly fed induction generator using back-to-back PWM converters supplying an isolated load from a variable speed wind turbine.* In: IEE Proc.-Electr. Power Appl., Vol. 143, No. 5, Sep. 1996, p. 380-387.
15. Càrdenas R., Peña R., Proboste J., Asher G., Clare J.: *MRAS observer for sensorless control of standalone doubly fed induction generators.* In: IEEE Tans. Energy Convers., Vol. 20, No. 4, Dec. 2005, p. 710-718.
16. Mohamed M.B., Jemli M., Gossa M., Jemli K.: *Doubly fed induction generator (DFIG) in wind turbine. Modeling and power flow control.* In: Proc. IEEE Int. Conf. Ind. Technology ICIT'2004, p. 580-584.
17. Xin-fang Z., Da-ping X., Yi-bing L.: *Predictive functional control of a doubly fed induction generator for variable speed wind turbines.* In: Proc. 5th World Congress Intelligent Control and Automation, Hangzhou. P.R. China, June 15-19, 2004, p. 3315-3319.
18. Hadef M., Rekioua T., Mekideche M.R., Rekioua D.: *Direct torque and vector control of permanent magnet synchronous motor*. In: 4th Int. Conf. Elec. Engineering CEE'06, Batna, Algeria, Nov. 7-8, 2006, p. 368-372.
19. Golea A., Golea N., Kadjoudj M., Benounnes N.: *Computer aided design of sliding mode control of permanent magnet synchronous motor*. In: IEEE Proc., Int. Symposium Computer Aided Control Syst. Design, Hawaii, USA, Aug. 22-27, 1999, p. 602-606.
20. Rebouh S., Kaddouri A., Abdessemed R., Haddoun A.: *Nonlinear controller design for a permanent magnet synchronous motor.* In: IEEE Conf., 2007, p. 776-780.
21. Gayed A., Benkhoris M.F., Siala S., Ledoeuff R.: *Time-domain simulation of discret sliding control of permanent magnet synchronous motor.* In: IEEE, 1995, p. 754-759.